IOPscience iopscience.iop.org

Home Search Collections Journals About Contact us My IOPscience

An electronic structure study of single native defects in beta -SiC

This article has been downloaded from IOPscience. Please scroll down to see the full text article.

1993 J. Phys.: Condens. Matter 5 891

(http://iopscience.iop.org/0953-8984/5/7/016)

View the table of contents for this issue, or go to the journal homepage for more

Download details:
IP Address: 171.66.16.159
The article was downloaded on 12/05/2010 at 12:54

Please note that terms and conditions apply.

J. Phys.: Condens. Matter 5 (1993) 891–898. Printed in the UK

An electronic structure study of single native defects in β-SiC

Lu Wenchang†‡, Zhang Kaiming†‡ and Xie Xide†‡

† China Centre of Advanced Science and Technology (World Laboratory), PO Box 8730, Beijing, People's Republic of China
‡ Physics Department, Fudan University, Shanghai 200433, People's Republic of China

Received 10 September 1992, in final form 14 November 1992

Abstract. The linear muffin-tin orbital method in the tight-binding representation is adopted to study the electronic structures of the native defects in β-SiC with the Green function approach. The original potential parameters are obtained by the standard band calculation of bulk β-SiC and the change in the potential parameters is obtained self-consistently. It is found that the silicon vacancy acts as an acceptor and the carbon vacancy acts as a donor with the split-off states at 0.45 and 1.67 eV above the valence band maximum. For the antisite defects, there is no split-off state in the band gap.

1. Introduction

Silicon carbide is a useful material for high-temperature and high-frequency electronics because of its large band gap (2.2 eV at room temperature), high drift velocity, temperature stability and chemical inertness [1]. Because of the development of the chemical vapour deposition (CVD) and molecular beam epitaxy (MBE) techniques, it is possible to grow high-quality crystals of zincblende-structure silicon carbide (β-SiC). Generally, CVD-grown β-SiC is Si rich and MBE-grown β-SiC can be made either Si rich or C rich. The deviation from stoichiometry is about 0.1%. Although this deviation is small, it may result in a high concentration of native defects, such as vacancies, antisites and self-interstitial defects. The understanding of the electronic structures of these native defects is important to improve the doping efficiencies of acceptors [2, 3]. The present paper is devoted mainly to studies on the electronic structures of single native defects in β-SiC.

Recently, there has been a number of experimental studies on defects in β-SiC [4–7] and in α-SiC [8, 9], but the interpretations of the experimental data differ significantly. For example, Nagesh *et al* [4], using deep-level transient spectroscopy (DLTS), have found that an epitaxial β-SiC film is free of deep-level defects in the upper third of the band gap and that most of the defects produced during neutron irradiation are confined to the lower two thirds of the band gap. However, Zhou *et al* [5], using the same method, have found two deep levels located at 0.34 and 0.68 eV below the bottom of the conduction band. Freitas and Bishop [7] have investigated the temperature and excitation intensity dependence of photoluminescence (PL) spectra in several undoped and lightly Al-doped thin films of β-SiC grown by CVD on an Si substrate and found a deep acceptor located at 0.47 eV above the top of the valence band. Their group has also studied the PL spectra of β-SiC films implanted with B, P and Al.

0953-8984/93/070891+08$07.50 © 1993 IOP Publishing Ltd

Several theoretical investigations of defects in β-SiC have been reported in recent years. Kohyama *et al* [10, 11] have studied the atomic and electronic structures of polar and non-polar grain boundaries in β-SiC, using the self-consistent tight-binding (TB) method. Cheng *et al* [12] have investigated boundary–boundary interactions of SiC. Lambrecht and Segall [13] have studied the (110) inversion domain boundary in β-SiC using the linear muffin-tin orbital (LMTO) method. Roberson and Estreicher [14] have calculated the electronic structures of neutral interstitial hydrogen in various polytypes of SiC using the method of partial retention of diatomic differential overlap. The electronic structures of the native defects have been calculated by several workers [15–17]. Using a large-cluster recursion method within the framework of the TB approximation, Yuan Li and Lin-Chung [15] have found that C and Si vacancies in β-SiC will behave as acceptors and donors, respectively. However, Talwar and Feng [17], using the Green function (GF) method within the TB approximation, have found that the C and Si vacancies in β-SiC will behave as donors and acceptors, respectively. Wang *et al* [16], using a supercell pseudopotential calculation, have observed the same behaviour as did Talwar and Feng. In this paper, we use the LMTO method with the GF approximation to study the electronic structures of native defects in β-SiC.

The paper is organized as follows. The calculation method and formula are presented in section 2. The electronic structures of native defects are discussed in section 3, and a summary is given in section 4.

2. Calculated method and formula

Among the existing calculations for impurities and defects, some are first-principles calculations based on a cluster or supercell approach and some are made using the semiempirical TB method with the GF approach. Gunnarsson *et al* [18] have developed a GF matrix technique based on the LMTO method within the atomic sphere approximation. In such an approach, first the GF of the perfect crystal can be obtained by a standard LMTO band calculation, and then the defects are treated as a perturbation to the perfect crystal and the perturbed GFs are obtained by solving the Dyson equation. Skriver and Rosengaard [19] have implemented an efficient self-consistent GF technique for calculating the ground-state properties of surfaces and interfaces, based on the LMTO method with the TB representation (TB-LMTO). In the present paper, we adopt the TB representation of the LMTO method to generate infinite-crystal GFs and then calculate the electronic structures of defects. Since the interaction between atoms is extremely short ranged in the TB representation, only a few atoms around the defect site should be treated self-consistently via the Dyson equation.

2.1. TB representation of LMTO and GF method

Within a nearly orthogonal muffin-tin orbital representation [20], one can write the Hamiltonian matrix elements in Bloch representation as

$$H_{iL,jL'}(k) = C_{iL}\delta_{ij}\delta_{LL'} + \sqrt{\Delta_{iL}}S_{iL,jL'}(k)\sqrt{\Delta_{jL'}} \tag{1}$$

where i and j are the atomic labels in a unit cell, and L and L' are orbital labels of the atoms. C_{iL} and Δ_{iL} are the band centre and band width of the Lth orbital of

the ith atom; their values are taken from the self-consistent bulk calculation by the standard LMTO method. The orthogonal structure constant $S(\boldsymbol{k})$ can be calculated in three steps. First, one can calculate the TB structure constant matrix $\mathbf{S}^{\beta}$ in real space by solving the Dyson equation [20]

$$S^{\beta}_{RiL,R'jL'} = S^{0}_{RiL,R'jL'} + \sum_{R''mL''} S^{0}_{RiL,R''mL''} \beta_{L''} S^{\beta}_{R''mL'',R'jL'} \quad (2)$$

where the sum is taken over all atoms and orbitals. $\mathbf{S}^0$ are unscreened structure constants and the explicit expressions for $\mathbf{S}^0$ may be found in [21]. The diagonal screening matrix elements $\beta_{L''}$ are chosen to be 0.3485, 0.05303 and 0.010714 for s, p and d orbitals, respectively, as in the literature [19]. This choice makes the structure constants $\mathbf{S}^{\beta}$ so localized that the lattice summation in equation (1) is only over the nearest-neighbour (NN) and the next-nearest-neighbour atoms. Then, using the Bloch sum, the TB structure constant $\mathbf{S}^{\beta}(\boldsymbol{k})$ in reciprocal space can be obtained. Finally, the orthogonal structure constants in reciprocal space are calculated from the Dyson equation [21]:

$$S_{iL,jL'}(\boldsymbol{k}) = S^{\beta}_{iL,jL'}(\boldsymbol{k}) + \sum_{mL''} S^{\beta}_{iL,mL''}(\boldsymbol{k})(\gamma_{mL''} - \beta_{L''}) S_{mL'',jL'}(\boldsymbol{k}) \quad (3)$$

where the summation extends over all atoms in a unit cell and their orbitals; $\gamma_{mL''}$ are the potential parameters related to the radial wavefunction of the atom m and its energy derivative [22] and can be taken from the standard band LMTO calculation. Then, one can solve the Schrödinger equation

$$[H(\boldsymbol{k}) - E(\boldsymbol{k})]u(\boldsymbol{k}) = 0 \quad (4)$$

and obtain the eigenvalues $E_n(\boldsymbol{k})$ and wavefunction $u_n(\boldsymbol{k})$. The infinite-crystal GF matrix elements in the reciprocal space can be obtained from

$$G^{0}_{iL,jL'}(\boldsymbol{k}, E) = \sum_{n} \frac{u^{n}_{iL}(\boldsymbol{k}) u^{n}_{jL'}(\boldsymbol{k})^{*}}{E - E_n(\boldsymbol{k}) - \mathrm{i}0^{+}} \quad (5)$$

where the summation extends over all energy levels. In real space, the GF matrix elements become

$$G^{0}_{RiL,R'jL'}(E) = \frac{1}{V_{\mathrm{BZ}}} \int \mathrm{d}\boldsymbol{k}\, \exp[-\mathrm{i}\boldsymbol{k} \cdot (\boldsymbol{R} + \boldsymbol{r}_i - \boldsymbol{R}' - \boldsymbol{r}_j) G^{0}_{iL,jL'}(\boldsymbol{k}, E). \quad (6)$$

In the calculation, the imaginary parts of the GF matrix elements are calculated by means of the tetrahedron technique [23], and a grid of 89 $\boldsymbol{k}$-points in the irreducible Brillouin zone of the face-centred cubic structure is taken. The real parts of the GF matrix elements are obtained from the dispersion relation

$$\mathrm{Re}[\mathbf{G}^0(E)] = \frac{1}{\pi} \mathcal{P} \int \frac{\mathrm{Im}[\mathbf{G}^0(\omega)]}{E - \omega} \mathrm{d}\omega \quad (7)$$

where $\mathcal{P}$ indicates the principal value of the integral.

From the GF, one can obtain the projected density of states (DOS)

$$N_{RiL}(E) = (1/\pi)\,\mathrm{Im}[G_{RiL,RiL}(E)]. \tag{8}$$

The iteration process is the same as in the standard LMTO method [22]. The first-order moments of the DOSs are evaluated from

$$M_{iL} = \int_{\infty}^{E_F} (E - E_{\nu iL}) N_{RiL}\,\mathrm{d}E. \tag{9}$$

The self-consistent criterion is that the first-order moments vanish. In that case, $E_{\nu iL}$ is the centre of gravity of the occupied part of the iL band. In the standard band calculation, convergence occurs when the sum of the absolute values of the first-order moments of the DOSs ($\sum_{iL}|M_{iL}|$) is less than 10^{-5}. If the same potential parameters are used in the TB-LMTO calculation, this sum is less than 10^{-4}. Therefore the accuracy of the TB-LMTO method is quite satisfactory.

2.2. *Application to defects*

To perform the self-consistent calculation for defects and impurities, it is convenient to define the other type of GF as follows:

$$[\mathbf{P}(E) - \mathbf{S}^{\beta}]\mathbf{g}^0(E) = 1 \tag{10}$$

where elements of the diagonal matrix $\mathbf{P}(E)$ are defined by

$$P_{RiL,R'jL'}(E) = \{(E - C_{iL})/[(E - C_{iL})(\gamma_{iL} - \beta_L) + \Delta_{iL}]\}\delta_{RR'}\delta_{ij}\delta_{LL'}. \tag{11}$$

We can find the relation between the GFs $\mathbf{g}^0$ and $\mathbf{G}^0$ through the following equation:

$$\begin{aligned} g^0_{RiL,R'jL'}(E) = {} & (\beta_L - \gamma_{iL})\{[(E - C_{iL})(\gamma_{iL} - \beta_L) + \Delta_{iL}]/\Delta_{iL}\}\delta_{RR'}\delta_{ij}\delta_{LL'} \\ & + \{[(E - C_{iL})(\gamma_{iL} - \beta_L) + \Delta_{iL}]/\Delta_{iL}\}G^0_{RiL,R'jL'} \\ & \times \{[(E - C_{jL'})(\gamma_{jL'} - \beta_{L'}) + \Delta_{jL'}]/\Delta_{jL'}\}. \end{aligned} \tag{12}$$

Because of the introduction of defects and impurities, the diagonal matrix $\mathbf{P}(E)$ of the perturbed sites will change to $\mathbf{P}(E) + \delta\mathbf{P}(E)$. If we do not consider the distortion of the lattice, the perturbed GF $\mathbf{g}$ is given by the Dyson equation

$$\mathbf{g}(E) = \mathbf{g}^0(E) + \mathbf{g}^0(E)\delta\mathbf{P}(E)\mathbf{g}(E). \tag{13}$$

The perturbed GFs $\mathbf{g}$ and $\mathbf{G}$ have the same relation as the perfect GFs $\mathbf{g}^0$ and $\mathbf{G}^0$ (see equation (12)). Therefore we can obtain the perturbed GFs $\mathbf{G}$ from equations (12) and (13) and then the projected DOS $N_{RiL}(E)$ from equation (8).

The iteration process for calculating $\delta\mathbf{P}(E)$ is the same as in the standard LMTO method except for the change in the Madelung potential. Because of the introduction of defects and impurities, the charges on the perturbed region will be redistributed. The charge in the perturbed region will not be conserved, since there is also a small change in charge density outside this region. We assume that this change in charge is distributed on the NN of the perturbed sites [18]. The variation in Madelung potential at site $\boldsymbol{R}$ can be written as

$$\delta V_{\mathrm{M}}(\boldsymbol{R}) = \sum_{\boldsymbol{R}'}{}' \frac{2\delta q_{\boldsymbol{R}'}}{|\boldsymbol{R} - \boldsymbol{R}'|} \tag{14}$$

where $\boldsymbol{R}'$ runs over all the perturbed sites and their NN sites, and $\delta q_{\boldsymbol{R}'}$ is the change in charge on site $\boldsymbol{R}'$.

2.3. Split-off state in the band gap

After self-consistent calculation, the change $\delta \mathbf{P}(E)$ in the diagonal matrix can be obtained. In the band gap, the imaginary part of the unperturbed GF $\mathrm{Im}\,\mathbf{g}^0$ is equal to zero. From the Dyson equation (13), a split-off state at energy E_b in the band gap is determined by the equation

$$\det\{1 + \mathrm{Re}[\mathbf{g}^0(E_b)\delta \mathbf{P}(E_b)]\} = 0. \tag{15}$$

3. Results and discussion

The four single native defects in β-SiC, namely carbon vacancies, silicon vacancies, Si_C antisites (where a C atom is substituted by an Si atom) and C_{Si} antisites (where an Si atom is substituted by a C atom), are considered in the present work.

Wang *et al* [16] have investigated the relation around the defects. The NN atoms around the carbon vacancy relax by 0.6%; the relaxation of the atoms around the C_{Si} antisite defect is inwards and the relaxation for the Si_C antisite defect is outwards. In the present paper, the relaxation is not considered, and the results are in agreement with those of Wang *et al* [16]. In addition, we consider only the neutral charge state of the defects.

The original potential parameters are obtained from the standard band calculation of bulk β-SiC and the perturbed potential parameters are obtained self-consistently. In our calculation, the perturbed sites include three shells: the first shell is the defect site, the second shell includes four NN real atoms and the third shell includes four NN empty atoms. The original and the perturbed potential parameters of the NN real atoms of the defect sites are listed in table 1. Comparing the perturbed potential parameters with the original parameters, we can see that the parameters Δ_{iL} change less than 5% and the parameters C_{iL} change less than 10% except for the parameter C_p (band centre of the p orbital of the NN carbon atom) for the C_{Si} antisite defect (about 14%). The changes in the potential parameters of the NN empty atoms are evaluated to be less than 3%. Therefore, it is sufficient to consider the perturbed sites to three shells.

Table 1. Perturbed potential parameters of the NN atoms of the defect sites. The values in parentheses are the original potential parameters.

	C_s (eV)	C_p (eV)	C_d (eV)	Δ_s (eV)	Δ_p (eV)	Δ_d (eV)
C_{Si}	−13.44	1.33	49.22	2.80	1.77	3.85
	(−13.04)	(1.54)	(49.37)	(2.83)	(1.78)	(3.81)
V_{Si}	−12.93	1.63	49.84	2.72	1.70	3.75
	(−13.04)	(1.54)	(49.37)	(2.83)	(1.78)	(3.81)
Si_C	−7.36	11.35	32.03	4.07	3.17	2.35
	(−6.79)	(11.83)	(32.27)	(4.03)	(3.13)	(2.28)
V_C	−6.88	11.75	32.23	4.04	3.14	2.30
	(−6.79)	(11.83)	(32.27)	(4.03)	(3.13)	(2.28)

The variation in the charge in NN empty spheres is very small for all the defects that we considered. For the C_{Si} antisite, the NN C atom loses about 0.25 electron. For the Si_C antisite, the NN Si atom gains 0.24 electron. The NN Si atom gains 0.05 electron for the carbon vacancy and the NN C atom loses 0.50 electron for the silicon vacancy owing to the absence of the cation Si.

Because of the underestimation of the band gap within the local-density approximation, the calculated fundamental band gap (Γ_{15v}–X_{1c}) in the present work (1.50 eV) is smaller than the experimental band gap (2.2 eV at room temperature) by about 32%. Using the self-energy correction of Bechstedt and Del Sole [24], which is in the form of rigid shift of the conduction band, the fundamental band gap is found to be 2.47 eV. This value is close to the experimental results. The split-off states in the band gap will be corrected by the Bechstedt–Del Sole method.

Because of the large difference between the electronegativities and core sizes of the silicon and carbon atoms, the electronic properties of β-SiC are similar to those of group III–V compound semiconductors, with the Si and C atoms acting in part as cations and anions, respectively. It is expected that the Si dangling-bond state of a carbon vacancy has a higher energy than the C dangling-bond state of a silicon vacancy. The present calculations show that the split-off states in the band gap for a silicon vacancy and a carbon vacancy are 0.35 eV and 1.67 eV respectively (measured from the valence band maximum). The values are comparable with the empirical TB calculation by Talwar and Feng [17]. They obtained 0.54 eV and 1.66 eV for silicon and carbon vacancies respectively. Silicon vacancies act as acceptors, and carbon vacancies act as donors, as we expected. These properties of vacancies in β-SiC are similar to those in group III–V compound semiconductors. However for Si_C and C_{Si} antisite defects, we do not find any split-off states in the band gap, which is different from the corresponding situation for the antisite defects in group III–V compound semiconductors. This might be because both the Si and the C atoms in β-SiC have four valence electrons whereas one atom has three valence electrons and the other atom has five valence electrons in group III–V compound semiconductors. The above results agree qualitatively with the pseudopotential calculation made with a supercell approach by Wang *et al* [16].

The local DOSs for an Si vacancy, a C vacancy, an Si_C antisite and a C_{Si} antisite are plotted in figures 1, 2, 3 and 4, respectively. The vertical line in each figure indicates the valence band maximum. In order to discuss the variation in the local DOSs, the local DOSs of the pure host atoms are shown in figure 5. The upper curves are the local DOSs for defect sites, and the lower curves are the local DOSs for the NN real atoms of the defects. For the silicon vacancy, there is a resonance state about 0.2 eV below the valence band maximum in addition to the split-off state in the band gap. For the carbon vacancy, there is a resonance state in the conduction band in addition to the split-off state in the band gap. A resonance state exists below the valence band maximum in the case of the Si_C antisite defect, and a resonance state exists above the conduction band minimum in the case of the C_{Si} antisite defect. Moreover, it is found that an s-like resonance state at about −7.0 eV exists for both Si_C and C_{Si} antisite defects.

Nagesh *et al* [4] found no deep levels in the upper third of the band gap using DLTS, but Zhou *et al* [5], using the same method, have found at least two deep levels, one of which is located 0.34 eV from the conduction band edge and the other is located 0.68 eV from the conduction band edge. If the corrected fundamental band gap of 2.47 eV is accepted, the second deep level observed by Zhou *et al* [5] is located

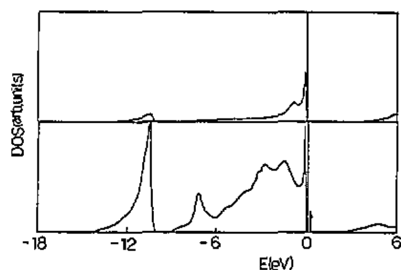

Figure 1. Local DOSs for a silicon vacancy. The upper curve is the local DOS of the defect site and the lower curve is the local DOS of the NN site of the defect. The arrow indicates the split-off state.

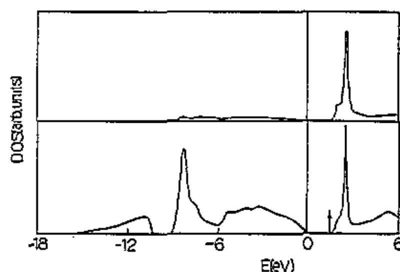

Figure 2. Local DOSs for a carbon vacancy. The upper curve is the local DOS of the defect site and the lower curve is the local DOS of the NN site of the defect. The arrow indicates the split-off state.

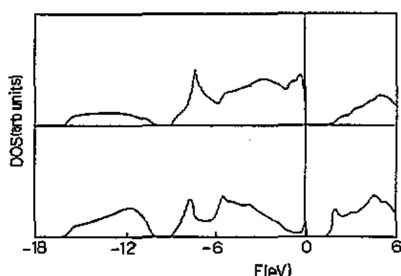

Figure 3. Local DOSs for the Si_C antisite defect. The upper curve is the local DOS of the defect site and the lower curve is the local DOS of the NN site of the defect.

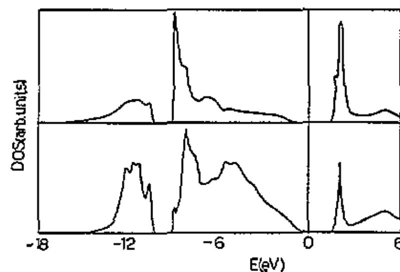

Figure 4. Local DOSs for the C_{Si} antisite defect. The upper curve is the local DOS of the defect site and the lower curve is the local DOS of the NN site of the defect.

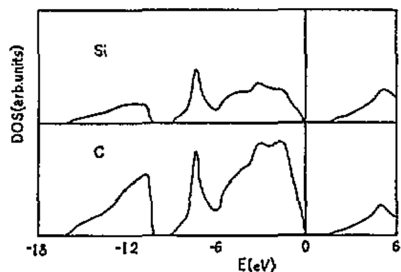

Figure 5. Local DOSs for the pure host atoms. The upper curve is for the pure host Si atom and the lower curve is for the pure host C atom.

1.79 eV above the valence band maximum. This value is comparable with the deep level (1.67 eV above the valence band maximum) induced by the carbon vacancy in the present calculation.

4. Summary

In summary, we have calculated the electronic structures of the native defects in β-SiC using the LMTO method in the TB representation and GF approach. The original potential parameters are obtained by the standard band calculation of bulk β-SiC and the changes in the potential parameters are obtained self-consistently as we have

outlined in section 2. It is found that silicon vacancies act as acceptors and that carbon vacancies act as donors, which is like the vacancies in group III–V compound semiconductors. The present results are in agreement with the pseudopotential calculation by Wang *et al* [16] and the TB calculation by Talwar and Feng [17] but are different from the large-cluster recursion calculation by Yuan Li and Lin-Chung [15]. The antisite defects do not induce any split-off states in the band gap and only induce resonance states in the valence band and the conduction band, which is unlike the situation in group III–V compound semiconductors. Moreover, the deep level induced by carbon vacancies is comparable with the deep trap observed by Zhou *et al* [5] using DLTS.

References

[1] *Landolt–Börnstein New Series* 1982 vol 17a, ed O Madelung, M Schulz and H Weiss (Berlin: Springer)
[2] Kim H J and Davis R F 1986 *J. Electrochem. Soc.* **133** 2350
[3] Yamanaka M, Daimon H, Sakuma E, Misawa S and Yoshida S 1986 *J. Appl. Phys.* **61** 599
[4] Nagesh V, Farmer J W, Davis R F and Kong H S 1987 *Appl. Phys. Lett.* **50** 1138
[5] Zhou P, Spencer M G, Harris G L and Fekade K 1987 *Appl. Phys. Lett.* **50** 1384
[6] Freitas J A Jr, Bishop S G, Edmond J A, Ryu J and Davis R F 1987 *J. Appl. Phys.* **61** 2011
[7] Freitas J A Jr and Bishop S G 1989 *Appl. Phys. Lett.* **55** 2757
[8] Chou S Y, Chang Y, Weiner K H, Sigmon T W and Parsons J D 1990 *Appl. Phys. Lett.* **56** 530
[9] Schneider J, Muller H D, Maier K, Wilkening W, Fuchs F, Dornen A, Leibenzeder S and Stein R 1990 *Appl. Phys. Lett.* **56** 1184
[10] Kohyama M, Kose S, Kinoshita M and Yamamoto R 1990 *J. Phys.: Condens. Matter* **2** 7809
[11] Kohyama M, Kose S, Kinoshita M and Yamamoto R 1990 *J. Phys.: Condens. Matter* **3** 7555
[12] Cheng C, Heine V and Needs R J 1990 *Europhys. Lett.* **12** 69
[13] Lambrecht W R and Segall B 1990 *Phys. Rev.* B **41** 2948
[14] Roberson M A and Estreicher S K 1991 *Phys. Rev.* B **44** 10578
[15] Yuan Li and Lin-Chung P J 1987 *Phys. Rev.* B **36** 1130
[16] Wang C, Bernholc J and Davis R F 1988 *Phys. Rev.* B **38** 12752
[17] Talwar D N and Feng Z C 1991 *Phys. Rev.* B **44** 3191
[18] Gunnarsson O, Jepsen O and Andersen O K 1983 *Phys. Rev.* B **27** 7144
[19] Skriver H L and Rosengaard N M 1991 *Phys. Rev.* B **43** 9538
[20] Andersen O K and Jepsen O 1984 *Phys. Rev. Lett.* **53** 2571
[21] Andersen O K, Jepsen O and Glotzel D 1985 *Highlights of Condensed-Matter Theory* ed F Bassani, F Fumi and M P Tosi (New York: North-Holland)
[22] Skriver H L 1984 *The LMTO Method* (Berlin: Springer)
[23] Jepsen O and Andersen O K 1971 *Solid State Commun.* **9** 1763
[24] Bechstedt F and Del Sole R 1988 *Phys. Rev.* B **38** 7710